Available online at www.sciencedirect.com

ScienceDirect

Procedia Structural Integrity 24 (2019) 559–568

Structural Integrity Procedia

www.elsevier.com/locate/procedia

AIAS 2019 International Conference on Stress Analysis

Characterization of equivalent acoustic sources to reproduce the acoustic field generated by engines on an aircraft fuselage

Venanzio Giannella[a]*, Riccardo Lombardi[b], Matteo Maria Pisani[a], Luigi Federico[c], Mattia Barbarino[c], Roberto Citarella[a]

[a]*Deptartment of Industrial Engineering, University of Salerno, via Giovanni Paolo II, Fisciano (SA), Italy*
[b]*Noesis Solutions, Gaston Geenslaan, Leuven, Belgium*
[c]*Italian Aerospace Research Centre (C.I.R.A), via Maiorise snc, Capua (CE), Italy*

Abstract

This work presents a general procedure to characterize equivalent acoustic sources to reproduce the sound pressure field generated by the engines on an aircraft fuselage. The procedure would allow to set up ground experimental tests on aircraft components, by means of distributed loudspeakers, to obtain their vibro-acoustic performances as if they were tested in flight conditions.
A FEM model of an aircraft fuselage mock-up was built up, comprising the structure, the internal acoustic cavities and the external air. The sound pressure field generated by the engines was considered as the reference solution, whereas an equivalent sound field, produced by distributed monopole sources surrounding the structure, was obtained by leveraging on the proposed Multi-Disciplinary Optimization (MDO) procedure.
The MDO procedure was based on the mutual interaction between the commercial codes Siemens NX, for the CAE/FEM simulations, and Noesis Optimus, for the optimization framework.

Keywords: Aircraft fuselage; MDO; optimization; BPF; FEM

* Corresponding author. Tel.: +089-96-4111; fax: +089-96-4111.
E-mail address: vgiannella@unisa.it

10.1016/j.prostr.2020.02.049

1. Introduction

The reduction of acoustic emissions and the improvement of cabin interior comfort are on the path of all major industries of the transport system, having a direct impact on customer satisfaction and, consequently, on the commercial success of new products. Topics to be tackled deal with computational, instrumentation and data analysis of noise and vibration of fixed wing aircrafts, rotating wing aircrafts, space launchers, allowing for aerodynamically generated noise, engine noise, sound absorption, cabin acoustic treatments, duct acoustics, active noise control and vibro-acoustic properties of materials (Citarella, 2018).

Nowadays, aeronautics industry requires several experimental tests during the designing processes that, very often, present huge costs and generally are not even simple to carry out accurately. In this work, a procedure to characterize a set of acoustic sources that replicate the sound field produced by the engines on an aircraft fuselage has been built up.

The reference theory to predict the noise radiated by propellers can be found in (Lighthill, 1952, 1954), in which the Lighthill's analogy was originally developed for unbounded flows. Such aero-acoustic analogy assumed that the turbulent flows could be modelled as homogeneous acoustic media in steady-state conditions, with the acoustic field imposed by quadrupole sources. That formulation was extended by Ffowcs Williams (Ffowcs Williams, 1969) to take into account vibrating solid surfaces, rephrasing Navier-Stokes equations introducing source terms composed by:

- quadrupole sources, generated by the turbulence of the fluid,
- dipole sources, caused by fluctuations of the fluid-structural interaction forces,
- monopole sources, generated by fluctuations of mass.

These theories do not provide indications about the sources positioning, that commonly, in far field, are located in correspondence of the geometrical central axis of the propellers, and usually characterized by means of CFD calculations. Unfortunately, these theories are inefficient under near field conditions, therefore, in more complicated cases, it is necessary to proceed numerically to determine type, number and position of the acoustic sources. Their proper characterization would allow to replicate the real acoustic pressure fields generated by the engines via simplified acoustic sources. By means of such procedures, the experimental tests involving the fuselage structure could be carried out either in an anechoic or semi anechoic environment, with the emulated acoustic field imposed by distributed loudspeakers. This would also allow to carry out vibro-acoustics assessments on aircraft structures avoiding the huge effort of flight experimental testing campaigns.

Similar approaches in which simplified acoustic sources were used to simulate more complex acoustic fields, e.g. the noise generated by rocket engines, can be found in (Casalino, 2009; Bianco, 2018; Barbarino, 2017, 2018).

2. Problem description

This work can be split in two main parts:

- the first part comprised the CAD/FEM modelling, in which a simplified FEM vibro-acoustic model of an aircraft fuselage was built up; such model, comprising the structure, internal acoustic cavities and external fluid, was used to perform the vibro-acoustic analysis of the fuselage when loaded with the sound pressure emitted by the engines.
- the second part comprised the set-up of the Multi-Disciplinary Optimization (MDO) procedure, with the aim of characterizing a given number of acoustic sources that can reproduce, in a simplified manner, the real external sound field imposed by the engines.

The rotating fans were considered as the noise contributors that create periodic low frequency loads on the fuselage at the known Blade-Passage Frequency (BPF). In particular, in this work the sound pressure calculated for the BPF was considered as the only contributor to the external overall low frequency noise. However, standing the general procedure built up in this work, no more difficulties would arise if considering different frequencies or further noise contributors.

The MDO procedure was set up as an integrated modelling approach based on a mutual interaction between the commercial codes Siemens NX Nastran 12.0 (Siemens, 2019), for the FEM simulations, and Optimus 2019.1 (Optimus, 2019a), for the optimization framework.

The goal of the work was not the accurate reproduction of the real fuselage response to the noise coming from the engines, but only the implementation and validation of a general MDO procedure to solve a complex optimization problem such as the one here proposed. Therefore, some simplifications were considered as a trade-off between a sufficiently accurate physical replication of the vibro-acoustic fuselage behaviour and an acceptable computational burden. It is worth noting that the MDO procedure here proposed required many FEM solutions of the current model to provide a stable solution. Some references about the adopted algorithms can be found in (Jones, 1998; Optimus, 2019b). More details are provided in the followings.

This description is divided in three main parts.

The first part comprises the CAD/FEM modelling for the vibro-acoustic characterization of the aircraft fuselage; fuselage sizes, materials, boundary conditions and loads are described in this part.

The second part comprises the parametrization of the so obtained FEM model and the inherent MDO optimization process description. The procedure is based on the determination of magnitudes and phases of the sound power, emitted by four monopole sources irradiating the fuselage external surfaces, in such a way to replicate the reference pressure field representative of a realistic noise emission by the engines.

The third part illustrates the results and the related discussion. The optimization result, hereinafter “Simulated Case” (SC) is presented and the related pressure field is compared with the reference data, hereinafter “Real Case” (RC), showing a satisfactory agreement.

3. CAD/FEM modelling

The CAD/FEM modelling was subdivided into three main sub steps.

The first sub step was the FEM modelling, started from the initial CAD model of Fig. 1, with the related subdivision in 2D structure, 1D structure and internal fluid cavities, see Fig. 2.

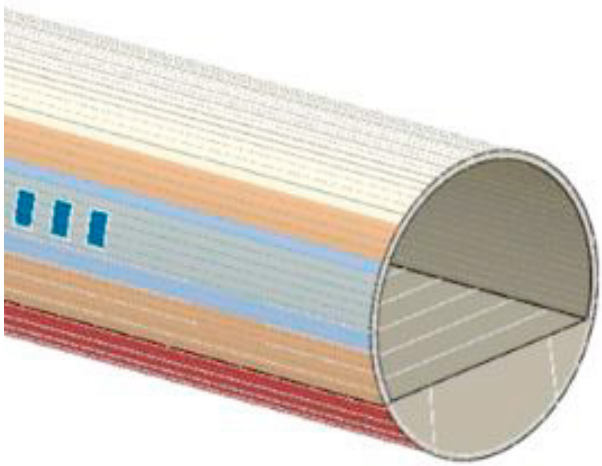

Fig. 1. CAD model of the aircraft fuselage.

The 2D structural part represented the key contributor to the vibration response of the model, and comprised four main surfaces made out of different materials (Fig. 2a):

- grey surface, representing the external surface on which the acoustic load impacts;
- orange surface, representing the lining panel, generally made out of a sandwich suitable to realize a noise and vibration reduction apt to improve the comfort inside the cabin;
- blue surface, representing the floor on which seats are located (seats were not modelled in this work);

- light blue surfaces, representing the window glasses.

The 1D structural elements (Fig. 2b) were divided in: longerons and circumferential beams to stiffen the structure, transversal and axial floor support, formed by beams with different sections, windows frameworks and doors. Furthermore, the sandwich was linked to axial and circumferential beams by elastic and rigid constraints.

The internal fluid cavities can be split in three parts (Fig. 2c): that inside the fuselage occupied by passengers, that occupied by the stowage under the floor, and that displaced between the external surface and the internal lining panels.

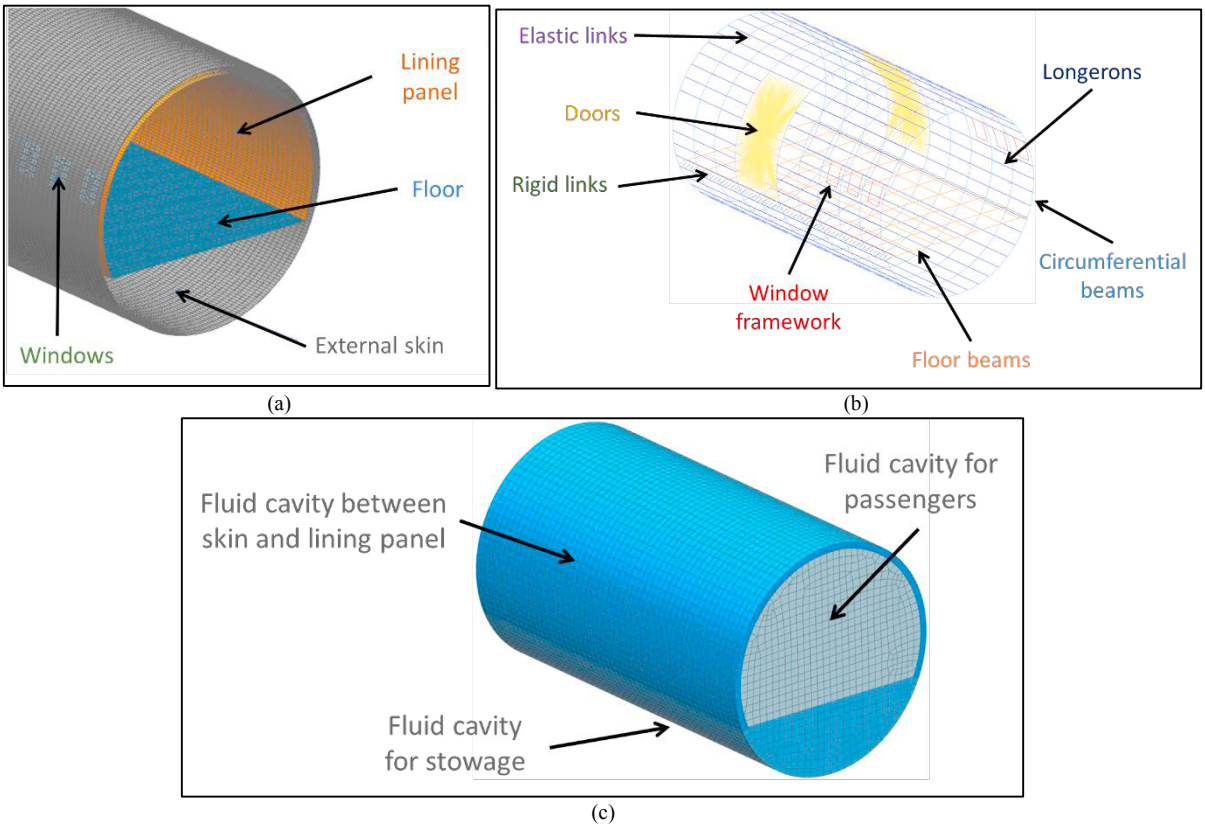

Fig. 2. FEM model subdivision: 2D (a) and 1D (b) structural elements; (c) internal fluid cavities.

The second sub step consisted into the modelling of the external fluid (Fig. 3), essential to measure the Acoustic Intensities (AIs) in 30 different microphone locations (5 rings of 6 microphones each) outside the fuselage external surface. Such part was modelled as a cube of solid elements with a hollow space in the centre to accommodate the fuselage structural model. Such cube was modelled with a size large enough to comprise at least 2 wavelengths at the frequency of interest. This was required in order to prevent boundary effects since the condition of infinite radiation was applied at the boundaries. The mesh comprised tetrahedral solid elements with variable size but with at least 6 nodes per wavelength, in order to have an accurate fluid field calculation in the fluid-structure interface zone (close to the structure), whereas larger elements were adopted far from the structure in order to reduce the computational burden.

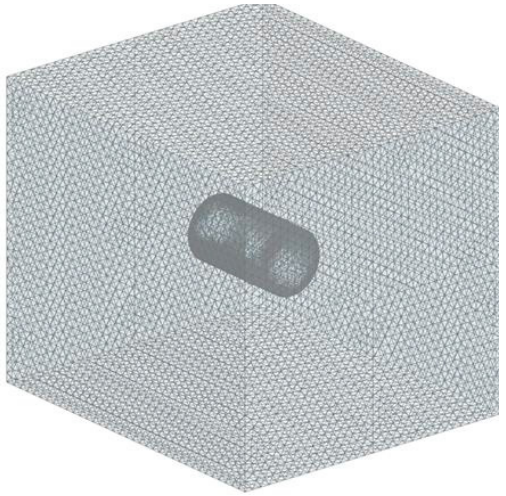

Fig. 3. External fluid mesh.

The third sub step comprised the definition of boundary conditions and loads for the FEM model.

Two different types of acoustic loads were considered for the Real Case (RC) and the Simulated Case (SC). In the former, the sound pressure field on the external fuselage surface (Fig. 4) was obtained by aero-acoustic simulations, considering as a noise source the rotating fans of the turboprops at the BPF. From Fig. 4, it can be noticed the load shape caused by the phase shift of the fans, and the increment of the load amplitude in the axial direction, as a consequence of the distance from the fan position.

In Fig. 5a the microphone positions are shown: they are needed to monitor the pressure field on the fuselage surface, used as input for the optimization algorithm. The turboprop fan positions represented a key element to properly locate the equivalent acoustic sources for the Simulated Case (SC), where four monopole acoustic sources (modelled with the ACSRCE card in the FEM code; Siemens, 2019) were introduced at positions shown in Fig. 5b.

The same constraints were used for both RC and SC: they can be subdivided in structural, fluid and fluid-structure coupling conditions. A fully clamped condition (Fig. 6a) was imposed at the two ends of the fuselage barrel analyzed (no translations neither rotations allowed). Two types of boundary conditions were set up for the fluid: the two fuselage ending surfaces were considered as acoustically rigid (no interaction between internal and external fluids) whereas the six faces of the cube of the external fluid were modelled as anechoic walls (no reflection was allowed), using the Acoustically Matched Layer (AML; Siemens, 2019). Finally, a strong coupling between fluids and structural nodes was set up (Siemens, 2019) to allow for a mutual interaction between structural and fluid elements.

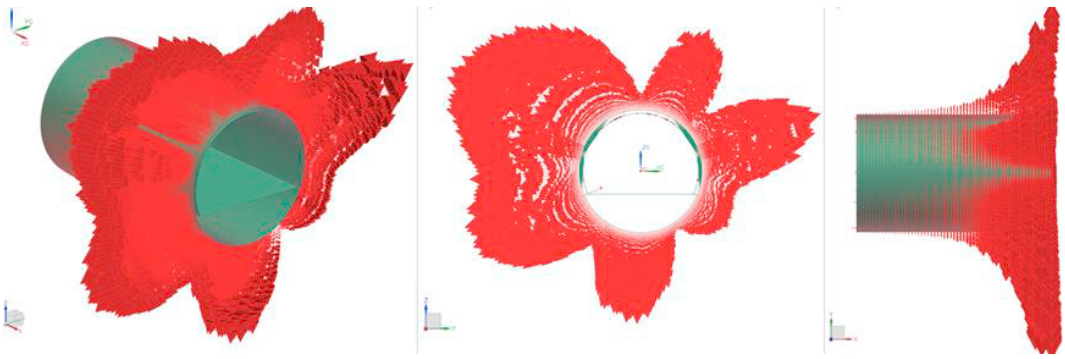

Fig. 4. Reference sound field considered as pressure load for the RC.

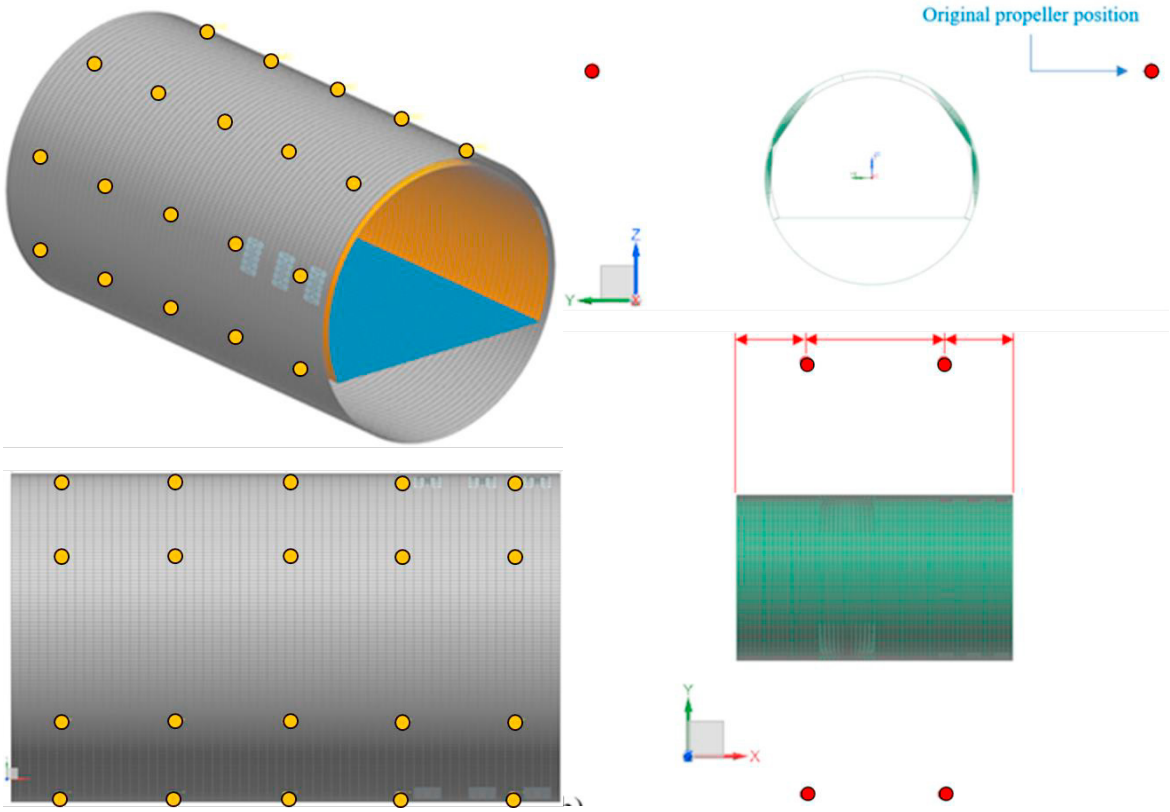

(a) (b)

Fig. 5. (a) Microphones positions (in yellow) and (b) monopole source positions (in red), representing the output and input positions for the optimization process respectively.

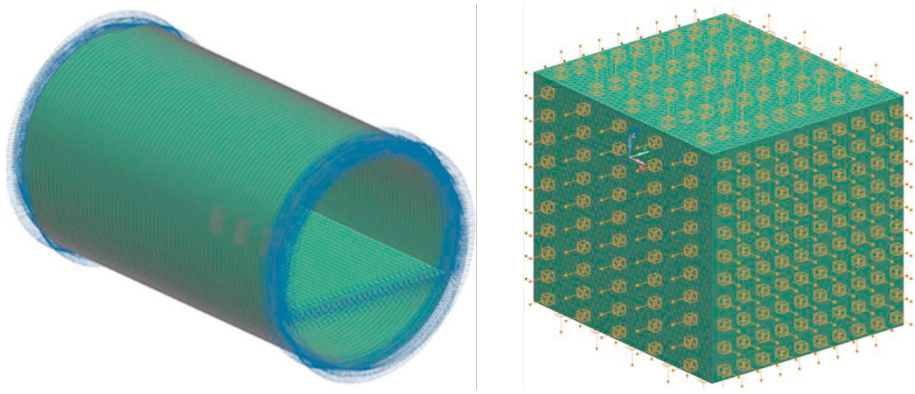

(a) (b)

Fig. 6. Boundary conditions: (a) clamped structural nodes, (b) non-reflecting boundary conditions.

Initial tentative sound power amplitude and phase were assigned for each monopole source; such values were then step by step adjusted by the optimization procedure.

A comparison between the cross sections (by a symmetry plane) of the final models built up for RC and SC is shown in Fig. 7.

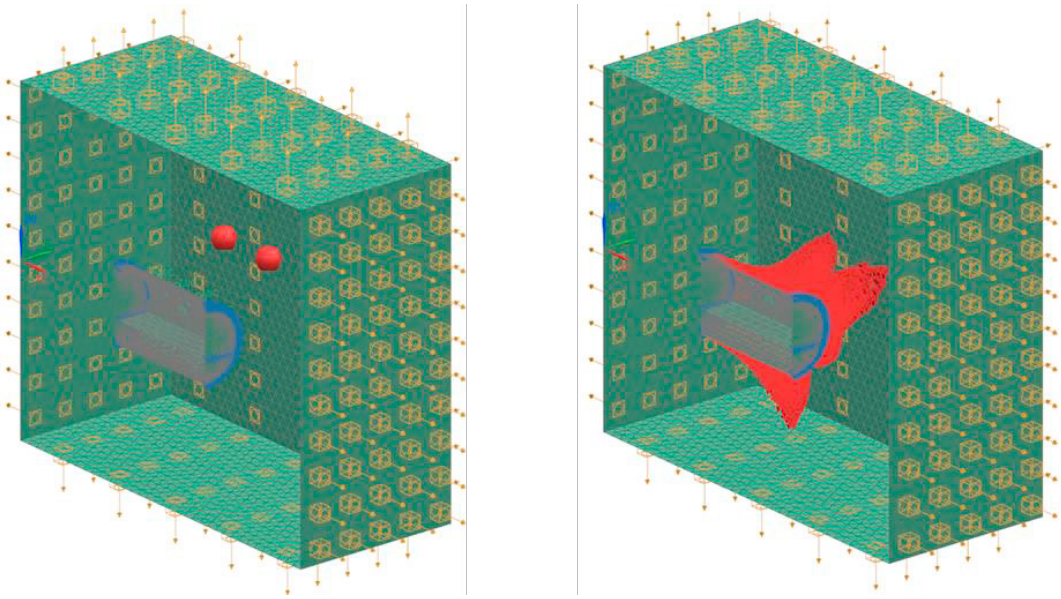

(a) (b)

Fig. 7. Cross section of the model adopted for (a) SC and the (b) RC respectively.

4. MDO optimization process

Sound power and phase of each monopole source represented the input data for the MDO process, whereas the acoustic intensities (AIs) at microphones provided the output. Thus, a parametrization of the model for the SC was required in order to change the input values for the FEM simulations and to get the output to compare with RC data. Such parametrization of the model was implemented in Optimus using the related interfaces after an appropriate set up of the FEM model.

The optimization strategy was an Efficient Global Optimization (EGO) derived methodology, simplified and customized in order to better drive the optimization algorithm to find a solution in such a complex optimization problem.

The MDO optimization procedure started with a Design Of Experiment (DOE), specifically the Latin Hypercube Design (LHD; Optimus, 2019b) was used for such a purpose to explore the variables domain. Consequently, the MDO optimization procedure proceeded by iterating the following steps:

- generation of a response surface, based on the DOE table data,
- run of the global optimization method on the response surface, to find a candidate point that minimizes the metrics,
- check of the proximity of the candidate point to the points considered in the previous iterations,
- space filling, to balance for the global optimization (based on surrogate models with known data) to fall into local minima without performing additional exploration,
- run the FEM analyses on the two new points,
- update the initial DOE data and iterate until a terminate criteria is satisfied.

Thus, the starting point of the MDO strategy is an existing DOE database, not necessarily tailored for optimization. Then, the global optimization method Differential Evolution (Storn, 1997), based on the Response Surface Method

(RSM) implemented through the use of Radial Basis Functions (RBFs), was performed to find a "good" candidate point (Optimus, 2019). It is worth noting that DEVOL was selected as global optimization method to guarantee a complete cover of the design space even if, generally, the downside is its computational burden. However, this was not a problem for the proposed procedure as the evaluation of hundreds of candidate points on the surrogate models is performed in sub-second time.

Subsequently, a proximity check was performed to avoid oversampling of the same design region and/or "cornered" RSMs, (measuring the distance between the proposed optimal point and the existing experiments) and a space filling was performed to improve the overall RSM and to reduce the chances of local minima traps (Van Dam, 2009). Instead of solving a complete MaxMin optimization problem, to determine the position in the design space of the experiment having the maximum/minimum distance from all the existing ones, a discretized version (based on a support LHD; McKay, 1979) was adopted to reduce the computational effort. As a final step, the FEM simulations for both candidate and "space filling" points were performed, and the results included in the DOE dataset to be used in the following iterations.

The graph shown in Fig. 8 was constructed in Optimus to run the MDO process.

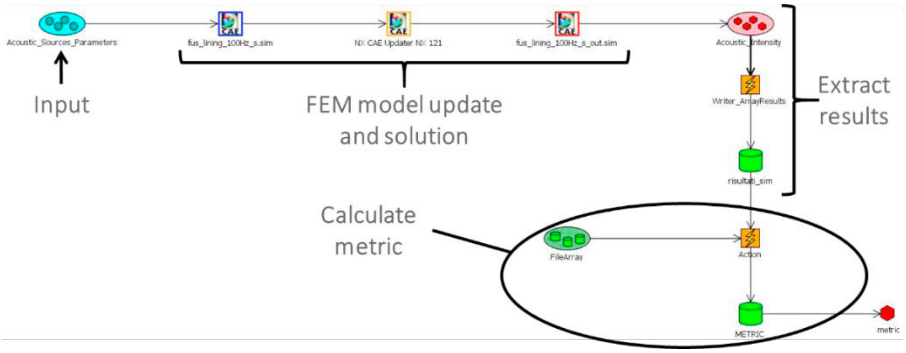

Fig. 8. Optimus graph to run the MDO process.

This optimization strategy made the structure flexible since the DOE results were independent from the chosen function for the metrics, i.e. the target function; the latter was defined in a python script loaded in the software (when calculating the metrics, see Fig. 8.

The choice of the metric function was a key point of the work in order to get the most appropriate comparison between RC and SC data. Some functions were tested and the final choice is reported in Eq. 1: it represents a normalized percentage difference among the AI values for each microphone:

$$metrics = \sum_{i=1}^{n} \left| \frac{AI_i^{RC} - AI_i^{SC}}{AI_i^{RC}} \right| \qquad \text{with } i = 1, 2, ..., n \tag{1}$$

, where n is the number of microphones, AI^{RC} is the acoustic intensity array for the RC, and AI^{SC} is the acoustic intensity array calculated for each iteration.

4. Results

The MDO procedure iterated on the sound powers and phases of the 4 monopole sources to obtain in the 30 microphones AIs as close possible to the AIs of the RC. After nearly 400 iterations the procedure stopped and the final comparison of the AIs at the microphone locations is shown in Fig. 9. Moreover, the whole pressure field on the external skin of the fuselage is also reported in Fig. 10, where the horizontal axis is the fuselage axis whereas the vertical axis is the angular coordinate around the fuselage.

The so obtained final metrics value was equal to 4.7%, stating that there was an average error between the reference and the obtained data of 4.7% for each microphone. Such error was judged as satisfactory, especially if considering the complexity of the study case here proposed for the presented optimization algorithm. The adoption of 4 monopole sources allowed to get a satisfactory correlation both along the tangential direction and along the axial direction of the fuselage mock-up.

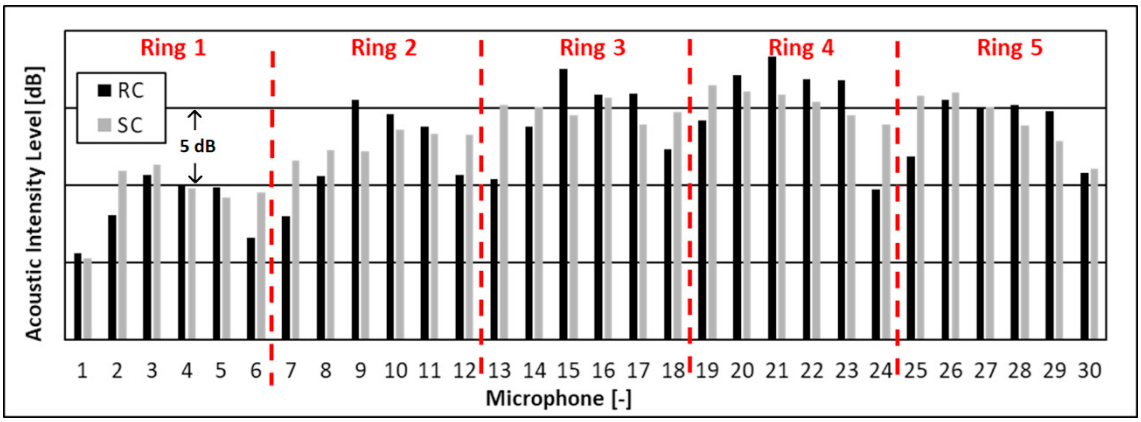

Fig. 9. AIs measured at the 30 microphones (5 rings of 6 microphones each) compared between RC and SC.

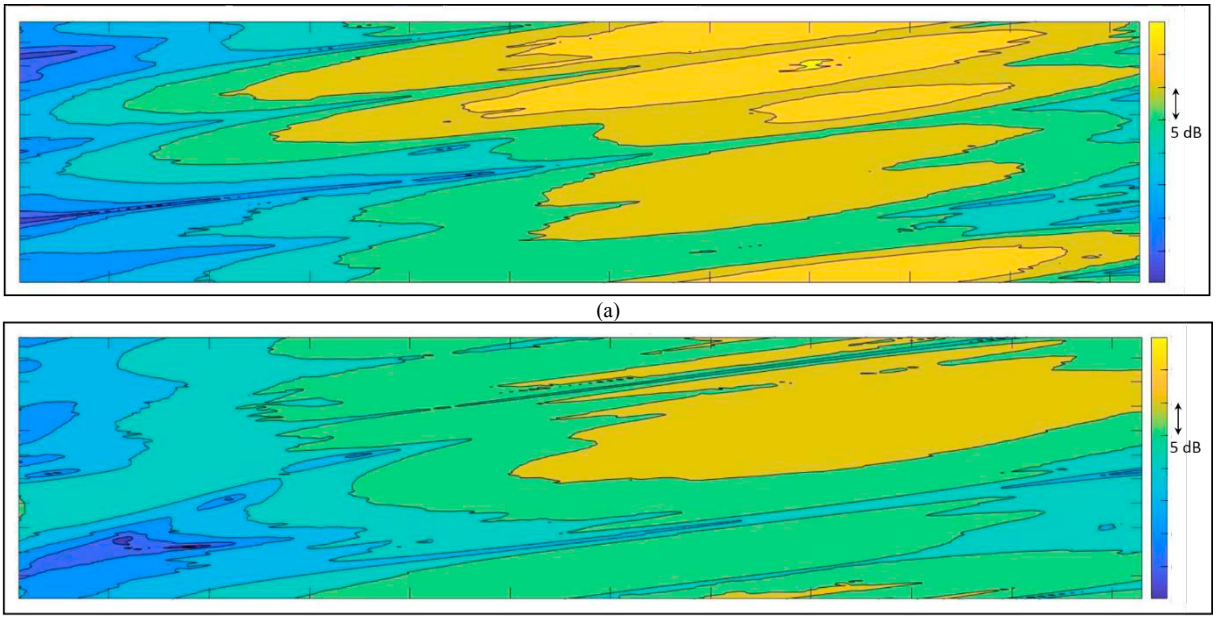

Fig. 10. Overall pressure field [dB] on the external skin compared between (a) RC and (b) SC.

4. Conclusions

A custom-made numerical optimization procedure has been set up to characterize acoustic sources to replicate the noise emitted by the aircraft engines during flight. Such a procedure enabled the setup of ground experimental tests

on a fuselage mock-up by means of distributed loudspeakers, in order to obtain its vibro-acoustic performance as in flight conditions.

A vibro-acoustic FEM model has been used to compute the vibrational response of the mock-up. Such FEM model has been then used as input model for the MDO strategy, allowing to characterize the loudspeakers emissions in terms of sound powers and phases. The comparisons between the reference and the so obtained pressure distributions are in a satisfactory agreement.

The set up procedure can be used as a reference tool to design simplified tests of more complex ones.

References

Barbarino, M., Adamo, F.P., Bianco, D., Bartoccini, D., 2017. Hybrid BEM/empirical approach for scattering of correlated sources in noise prediction, Journal of Sound and Vibration 403, 90-103.

Barbarino, M., Bianco, D., 2018. A BEM–FMM approach applied to the combined convected Helmholtz integral formulation for the solution of aeroacoustic problems. Computer Methods in Applied Mechanics and Engineering 342, 585-603.

Bianco, D., Adamo, F.P., Barbarino M., Vitiello, P, Bartoccini, D., Federico, L, Citarella, R., 2018. Integrated aero-vibroacoustics: the design verification process of Vega-C launcher, Applied Sciences, 8(1), 88.

Casalino, D., Barbarino, M., 2009. Hybrid Empirical/Computational Aeroacoustics Methodology for Rocket Noise Modeling, AIAA Journal 47(6), 1445- 1460.

Citarella, R., Federico, L., 2018. Advances in Vibroacoustics and Aeroacustics of Aerospace and Automotive Systems, Appl. Sci. 8, 366.

Ffowcs Williams, J.E., Hawkings, D.L., 1969. Sound Generation by Turbulence and Surfaces in Arbitrary Motion. Philosophical Transactions of the Royal Society of London. Series A, Mathematical and Physical Sciences 264, 321-342.

Jones, D.R., Schonlau, M., Welch, W.J., 1998. Efficient Global Optimization of Expensive Black-Box Functions. Journal of Global Optimization 13, 455-492.

Lighthill, M.J., 1952. On sound generated aerodynamically I. General theory. In: Proceedings of the Royal Society of London, Mathematical and Physical Sciences, A 221, 564-587.

Lighthill, M.J., 1954. On sound generated aerodynamically II. II. Turbulence as a source of sound. In: Proceedings of the Royal Society of London, Mathematical and Physical Sciences, A 222, 1-32.

McKay, M.D., Beckman, R.J., Conover, W.J., 1979. A Comparison of Three Methods for Selecting Values of Input Variables in the Analysis of Output from a Computer Code. American Statistical Association 21(2), 239–245.

Optimus 2019.1 – Users' Manual, 2019a. Noesis Solutions N.V.

Optimus 2019.1 – Theoretical Background for Optimus 2019b, Noesis Solutions N.V.

Siemens PLM Software Inc, 2019. Users' Manual, NX Nastran 12.0.

Storn, R., Price, K., 1997. Differential evolution - a simple and efficient heuristic for global optimization over continuous spaces. Journal of Global Optimization 11(4), 341–359.

Van Dam. E., den Hertog, D., Husslage, B., Rennen, G., 2009. http://www.spacefillingdesigns.nl/. Department of Econometrics and Operations Research, Tilburg University, The Netherlands.